Swiss J Geosci (2012) 105:67–84
DOI 10.1007/s00015-012-0092-6

Dating emplacement and evolution of the orogenic magmatism in the internal Western Alps: 2. The Biella Volcanic Suite

Notburga Kapferer · Ivan Mercolli · Alfons Berger · Maria Ovtcharova · Bernhard Fügenschuh

Received: 1 September 2011 / Accepted: 12 March 2012 / Published online: 29 April 2012

Abstract The high-pressure metamorphic rocks of the Sesia–Lanzo zone are partly covered by a volcano-sedimentary unit, the Biella Volcanic Suite. Calc-alkaline and shoshonitic lavas extruded sub-aerially on the Oligocene surface. Uranium–Lead zircon dating yields 32.44–32.89 Ma for the eruption of the calc-alkaline lavas and therefore fixes a minimum age for the paleosurface. The Biella Volcanic Suite consists mainly of epiclastic rocks deposited in a high-energy fluvial environment and minor lava flows. The rocks of the suite display widespread post-eruption transformations. Illite and chlorite thermometry as well as fission track dating suggest a thermal overprint related to burial of the Biella Volcanic Suite. An upper crustal rigid block tilting in the area causes this burial. Hydrothermal tourmaline and ankerite veins related to the intrusion of the nearby Valle del Cervo Pluton crosscut the already tilted Biella Volcanic Suite. The intrusion age of Valle del Cervo Pluton at 30.39 ± 0.50 Ma sets therefore the lower time limit for tectonic processes responsible for the tilting and burial. After the burial, the Biella Volcanic Suite remained for around 20 million years between the zircon and the apatite partial annealing zone. The apatite fission track ages spread between 16 and 20 Ma gives the time frame for the second exhumation of these units. The Biella Volcanic Suite and the adjacent rocks of the Sesia–Lanzo zone were the second time exhumed to the surface in Messinian times, after a long residence time within the apatite partial annealing zone.

Keywords Biella volcanic rocks · Sesia–Lanzo zone · U–Pb zircon dating · Fission track dating · Very low grade metamorphism

Editorial Handling: E. Gnos.

N. Kapferer · I. Mercolli
Institute of Geological Sciences, University of Bern, Baltzerstrasse 1+3, 3012 Bern, Switzerland

A. Berger (✉)
Department of Geography and Geology, University of Copenhagen, Øster Voldgade 10, 1350 Copenhagen, Denmark
e-mail: ab@geo.ku.dk

M. Ovtcharova
Section of Earth and Environmental Sciences, University of Geneva, Rue de Maraîchers 13, 1205 Geneva, Switzerland

B. Fügenschuh
Institute of Geology and Paleontology, University of Innsbruck, Innrain 52, 6020 Innsbruck, Austria

1 Introduction

The most internal part of the Sesia–Lanzo zone along the Canavese line is covered by a Tertiary volcano-sedimentary series. These rocks have been studied since long time following different perspectives (Bianchi and Dal Piaz 1963; Carraro 1966; Ahrendt 1969; Scheuring et al. 1974; Zingg et al. 1976; De Capitani et al. 1979; Lanza 1979; Callegari et al. 2004). Based on mineralogical and geochemical arguments on fresh samples, Callegari et al. (2004) described the origin and evolution of the volcanic suite. They called this unit the "Cover Series of the Sesia Zone". To emphasize its essentially volcanic origin and its restricted regional distribution, we suggest calling this unit the Biella Volcanic Suite (BVS). We intend to contribute to the precise dating of the emplacement and of the subsequent low temperature alteration during burial of these rocks. A dating approach was already presented in earlier

papers using K/Ar methods, which may be influenced by alteration of the rocks (Scheuring et al. 1974; Zingg et al. 1976). Such an overprint may include several steps of different alteration processes (ancient and modern surface weathering, syn-emplacement volcanic hydrothermal alteration, burial metamorphism). We tried to decipher this problem by combining the description of the mineralogical changes with radio-isotopic and fission track (FT) dating. The U/Pb system in zircon should not be strongly affected by such a low temperature overprint and have therefore the potential to record the crystallisation of zircon close to the eruption time of the magmas. In contrast, FT data are sensitive to thermal overprint and should give insights into the timing of the metamorphic overprint. Based on the combination of these two methods, we will propose a temporal scheme of the evolution of the BVS. The BVS is spatially and geochemically related to the coeval magmatic activity in this area, i.e., Valle del Cervo Pluton, Miagliano Pluton and Traversella Pluton (Fig. 1) and the numerous dykes intruding the rocks of the Sesia–Lanzo zone and Ivrea-Verbano zone. More detailed data on these plutonic rocks are given in a companion contribution (Berger et al. 2012b). The high precision time–temperature evolution of the BVS and related magmatic rocks will serve as a base to unravel the near surface tectonic evolution during Neogene times.

2 Geological setting

Oligocene, syn-orogenic volcanic and plutonic rocks outcrop together with high-pressure metamorphic rocks of the Sesia–Lanzo zone along a narrow region in the internal part of the Western Alps along the Canavese line (Fig. 1). The Canavese line is the western branch of the Periadriatic Lineament, a first order boundary in the Alps (e.g., Schmid et al. 1989). The Canavese line separates the Sesia–Lanzo zone from the Ivrea-Verbano zone (e.g., Ahrendt 1972, 1980; Schmid et al. 1987, 1989; Biino and Compagnoni 1989; Zingg and Hunziker 1990; Handy et al. 2005; Siegesmund et al. 2008). It forms a mylonite belt of variable thickness (10–300 m) of strongly deformed slices of rocks (cataclastic rocks, mylonites and locally fault gouge) derived from the Sesia–Lanzo, Ivrea-Verbano and Sesia Zones. Four major Alpine deformation events are superimposed on the different fault rocks along the Canavese line. In late Cretaceous to Paleocene times, a mylonite belt 1 (fault rocks 1 or mylonite belt 1 of Schmid et al. 1989) developed during subduction and exhumation of the Sesia–Lanzo zone. Further convergence in the Sesia–Lanzo zone produces new steeper Sesia-, Ivrea- and Canavese-derived mylonites (Schmid et al. 1987, 1989). This stage predates the emplacement of

Fig. 1 Geological map of the Biella area and profile along the Valle del Cervo. Compiled after: Malaroda et al. (1966); Bigioggero et al. (1994); Callegari et al. (2004); Rossetti et al. (2007); Zanoni et al. (2008); Wissmann (1985); Puschnik (2000); Caviezel (2007) and paleomagnetic data of dykes after Lanza (1977, 1979) ▶

volcanic rocks of the Biella Volcanic Suite on a preserved paleosurface on top of the gneisses of the Sesia–Lanzo zone (Schmid et al. 1989; Kapferer et al. 2011). From that moment, in the studied area, the Canavese line acts essentially as brittle fault system accommodating upper crustal tectonics (fault rocks 3 and 4; Berger et al. 2012a, b). The Sesia–Lanzo zone occurs to the northwest of the Canavese line, and consists of a poly-metamorphic fragment of continental crust derived from the Adriatic Plate (e.g., Dal Piaz 1999). It forms a lenticular body, oriented SW–NE, between the Canavese line in the south and the Piemonte ophiolite nappes to the north.

The investigated volcano-sedimentary rocks lie on top of the high-pressure rocks of the Mombarone nappe, part of the Sesia–Lanzo zone (Babist et al. 2006; more or less equivalent to "Eclogitic Micaschist Complex" of Compagnoni et al. 1977). The BVS are restricted to a narrow belt (ca. 20 km long and of variable thickness) along the above described Canavese line between the village of Donato and the upper Val Sessera (Fig. 1). Frequently, the epiclastic members of the volcanic suite contain components of the underlying rocks of the Sesia–Lanzo zone (Fig. 2; Bianchi and Dal Piaz 1963). The composition of the volcanic rocks ranges from basalt to andesite in the high-K calc-alkaline suite and from trachyandesite to trachydacite in the shoshonitic suite (Callegari et al. 2004). Bianchi and Dal Piaz (1963) characterized the volcano-sedimentary cover of the Sesia–Lanzo zone as a complex volcanic sequence of porphyries, coarse grained conglomerates, volcanic breccia and thin tuffitic layers. The epiclastic conglomerates form layered sequences of locally variable thickness (up to 400–500 m). The different layers are characterized by the variation of the grain size, the relative abundance of the different types of volcanic components and the variable amount and size of the Sesia clasts. Within such layers neither grading nor sorting of the components can be observed. Bianchi and Dal Piaz (1963) observed clasts of the eclogitic rocks from the Sesia–Lanzo zone within the volcano-sedimentary unit, and assumed a Permian age for the porphyries. Carraro (1966) described the basal layers of the epiclastic rock containing eclogitic clasts as a non-metamorphic psephitic continental series of upper Carboniferous age. In contrast, Scheuring et al. (1974) estimated a tertiary age for the volcaniclastic rocks based on paleobotanical data and K–Ar total rock ages of the andesitic volcanic rocks between 29 and 33 Ma.

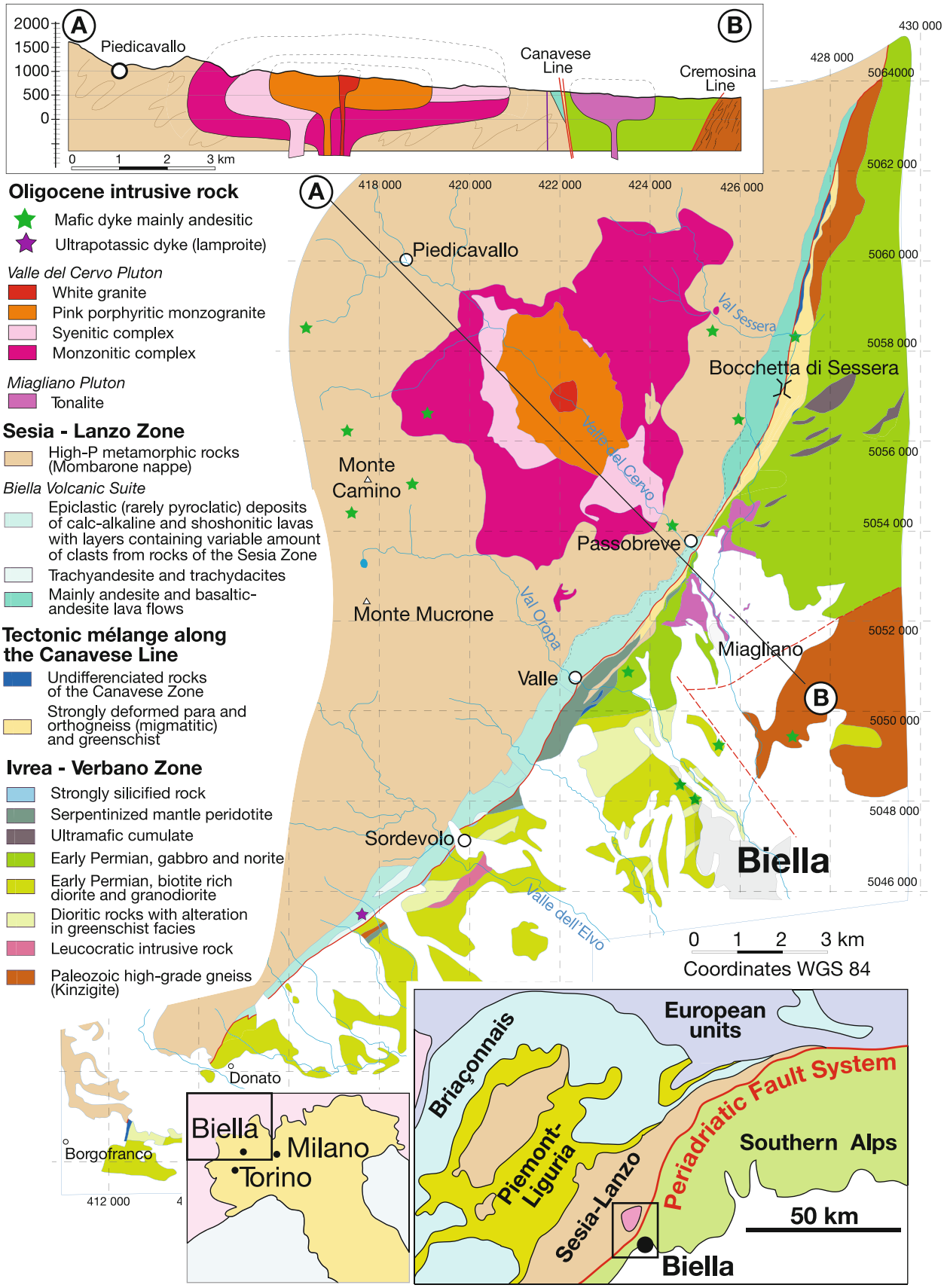
2000
1500
1000
500
0
A
B
Piedicavallo
Canavese Line
Cremosina Line
0 1 2 3 km
Oligocene intrusive rock
Mafic dyke mainly andesitic
Ultrapotassic dyke (lamproite)
Valle del Cervo Pluton
White granite
Pink porphyritic monzogranite
Syenitic complex
Monzonitic complex
Miagliano Pluton
Tonalite
Sesia - Lanzo Zone
High-P metamorphic rocks (Mombarone nappe)
Biella Volcanic Suite
Epiclastic (rarely pyroclastic) deposits of calc-alkaline and shoshonitic lavas with layers containing variable amount of clasts from rocks of the Sesia Zone
Trachyandesite and trachydacites
Mainly andesite and basaltic-andesite lava flows
Tectonic mélange along the Canavese Line
Undifferenciated rocks of the Canavese Zone
Strongly deformed para and orthogneiss (migmatitic) and greenschist
Ivrea - Verbano Zone
Strongly silicified rock
Serpentinized mantle peridotite
Ultramafic cumulate
Early Permian, gabbro and norite
Early Permian, biotite rich diorite and granodiorite
Dioritic rocks with alteration in greenschist facies
Leucocratic intrusive rock
Paleozoic high-grade gneiss (Kinzigite)
418 000
420 000
422 000
424 000
426 000
428 000
430 000
5064000
5062 000
5060 000
5058 000
5056 000
5054 000
5052 000
5050 000
5048 000
5046 000
Piedicavallo
Val Sessera
Bocchetta di Sessera
Valle del Cervo
Monte Camino
Passobreve
Monte Mucrone
Val Oropa
Miagliano
Valle
Sordevolo
Biella
Valle dell'Elvo
0 1 2 3 km
Coordinates WGS 84
Donato
Borgofranco
412 000
Biella
Milano
Torino
European units
Briançonnais
Piemont-Liguria
Sesia-Lanzo
Periadriatic Fault System
Southern Alps
50 km
Biella

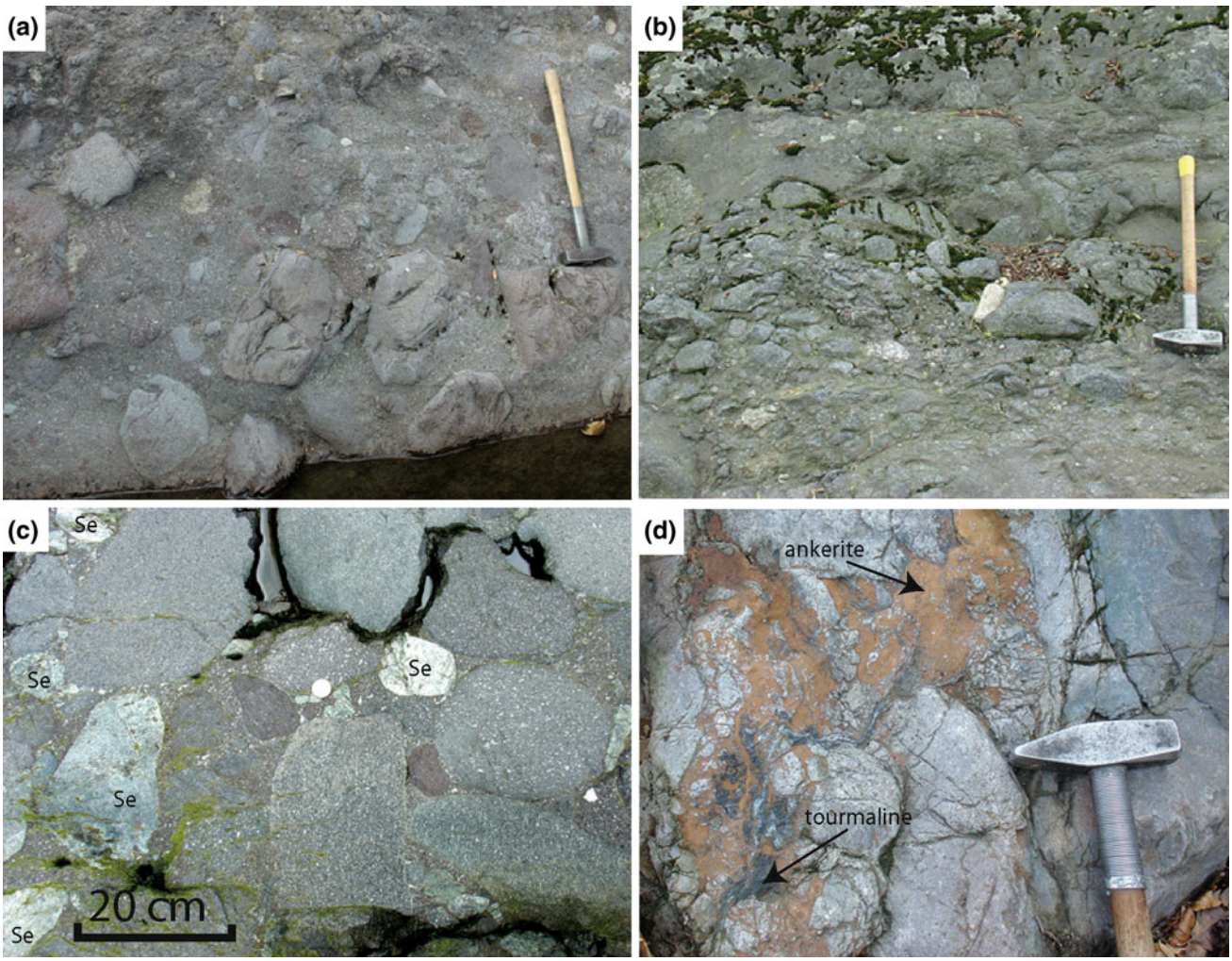

Fig. 2 Typical aspects of different lithologies in the BVS. **a** Epiclastic conglomerate with strong heterogeneous clasts size distribution (Valle, Val Oropa), **b** internal depositional layering in epiclastic conglomerate (Valle, Val Oropa), **c** epiclastic conglomerate with abundant clasts from the Sesia–Lanzo zone (Sordevolo), and **d** ankerite and tourmaline veins crosscutting andesitic epiclastite (Passobreve, Valle del Cervo)

3 Methods

The samples for zircon U/Pb dating have been crushed using the SelFrag (e.g., Giese et al. 2010) equipment at the University of Berne. After crushing, the zircons have been separated by sieving, Frantz magnetic separator, heavy liquid separation with bromoform and methylene iodide, and handpicking. Internal structures of the embedded and polished zircons were studied using SEM imaging at the Institute of Geology, University of Berne, to minimize the probability of inheritance and to detect inclusions. In order to minimize the effects of secondary lead loss the zircons were treated by "chemical abrasion" prior to analysis, involving high-temperature annealing followed by a HF leaching step (Mattinson 2005).

Annealing was performed by loading the zircon grains of each sample in quartz crucibles and placing them into a furnace at 900 °C for approximately 48 h. Subsequently, zircons from each sample were transferred into 3 ml screw-top Savillex vials together with ca. 120 µl concentrated HF and 20 µl 7 N HNO_3 for the leaching (chemical abrasion) step. Savillex vials were arranged into a Teflon Parr vessel with 2 ml concentrated HF, and placed in an oven at 180 °C for 12–15 h. After the partial dissolution step the leachate was completely pipetted out and the remaining zircons were rinsed in ultrapure water and then fluxed for several hours in 6 N HCl on a hotplate at a temperature of ca. 80 °C. After removal of the acid the fractions were again rinsed several times in ultra-pure water and acetone in an ultrasonic bath. Single zircons were selected, weighed and loaded for dissolution into pre-cleaned miniaturized Teflon vessels. After adding a mixed ^{205}Pb-^{233}U-^{235}U spike (EARTHTIME, spike calibration described by Condon et al. 2007) zircons were dissolved in 63 µl concentrated HF with a trace of 7 N

HNO3 at 206 °C for 6 days, then evaporated and the residue redissolved overnight in 36 µl 3 N HCl at 206 °C. Lead and Uranium from were separated by anion exchange chromatography (Krogh 1973) in 40 µl micro-columns, using minimal amounts of ultra-pure HCl and H_2O, and finally dried down with 3 µl of 0.06 N H_3PO_4. The isotopic analyses were performed in University of Geneva on a Thermo Scientific TRITON mass spectrometer equipped with a MasCom discrete dynode electron multiplier. The linearity of the multiplier was calibrated using U500, Sr SRM987, and Pb SRM982 and SRM983 solutions and found to be reproducibly at a dead time correction of 23.5 ns. The mass fractionation of Pb was controlled by repeated SRM981 measurements (0.13 ± 0.04 %/amu). Uranium mass fractionation is calculated in realtime using the ^{233}U-^{235}U ratio of the double spike solution. Both lead and uranium were loaded with 1 µl of silica gel–phosphoric acid mixture (Gerstenberger and Haase 1997) on outgassed single Re-filaments. Lead isotope compositions were measured on the electron multiplier, while U (as UO_2) isotopic measurements were made in static Faraday mode (using amplifiers equipped with 10^{12} Ω resistors) or, in case of insufficient U present-on the secondary electron multiplier. All common Pb in the zircon analyses was attributed to procedural blank and corrected with the following isotopic composition: $^{206}Pb/^{204}Pb$: 18.30 ± 0.71; $^{207}Pb/^{204}Pb$: 15.47 ± 1.03; $^{208}Pb/^{204}Pb$: 37.60 ± 0.98 (all 1 sigma %). Uranium blanks are <0.1 pg and do not influence the degree of discordance at the age range of the studied samples, therefore a value of 0.05 pg ± 50 % was used in all data reduction. As it is pointed out in several publications in the last few years, transparent error propagation and reporting the errors on each level (internal and external) is important for intercalibrating geochronologic data between different laboratories and different methods (Schoene et al. 2006; Schmitz and Schoene 2007; McLean 2011). The initial statistics was done using the TRIPOLI program (Bowring et al. 2011), followed by data reduction and age calculation using the PbMacDat program (applying the algorithm of Ludwig 1980). Generation of Concordia plots and averages was done with the Isoplot/Ex v3 program of Ludwig (2005). All uncertainties reported are at the two sigma level.

Observations were achieved using a Zeiss EVO 50 scanning electron microscope (SEM) and a Micro-Raman spectrometer. Minerals were analysed with a JEOL JXA-8200 electron microprobe at the University of Berne. Operating conditions for chlorite and clay measurements were 15 kV acceleration voltages, beam current of 8 nA and a 10 µm beam diameter, and with a beam current of 5 nA and a 7 µm beam diameter used for carbonates. The elements were measured for 20 s on the peak as well as the background. Natural and synthetic minerals were used as standards. For XRD analyses of chlorite and clay minerals, white-to-pale-green rock portions were selected by hand. The particles had previously been ground in the agate mortar to a clay-size fraction. Mixtures of powder and distilled water were dispersed ultrasonically, pipetted an air-dried on glass slides to produce thin-layered, orientated aggregates. In order to avoid the (partial) dissolution of chlorite, no acid treatment was applied. Glycosylation of an aliquot of the samples was undertaken for 8 hours at 50 °C for the detection of swellable minerals. X-ray diffraction analyses were undertaken with a Philips PW 1830 diffractometer using CuKα radiation (40 kV, 30 mA, divergence and detector slits of 0.02°, goniometer speed of 0.004°/s). The data analysis was performed using the X'Pert Quantify software, version 1.0c.

All fission track samples have been crushed using the SelFrag. After crushing, sieving, Frantz magnetic separator, heavy liquid separation with bromoform and methylene iodide, and hand picking) samples were mounted in epoxy resin (apatite) and PFA® Teflon (zircon). Revelation of fossil tracks was achieved by etching polished zircon mounts for 3–8 h in a NaOH–KOH eutectic melt at 235 °C. Apatite mounts were etched in 6.5 % HNO_3 at 20 °C for 40 s. Induced tracks in external detector muscovites were etched in 40 % HF for 45 min at 20 °C. Irradiation of both zircon and apatite was carried out at the FRM II research reactor in Garching, Germany. Neutron flux was monitored using CN1 (for zircon) and CN5 (for apatite) dosimeter glasses. Ages were calculated using the zeta calibration method (Hurford and Green 1983) with a zeta factor of 190.2 ± 9.0 (zircon, CN1 glass) and 357.7 ± 39.8 (apatite, CN5 glass). Durango apatite (31.4 ± 0.5 Ma) and Fish Canyon Tuff apatite and zircon (27.9 ± 0.5 Ma) were used as international age standards for the zeta calibration. Samples were analysed using the external detector method as described by Gleadow (1981). The measurements were carried out using a Zeiss Axio Imager A1 m microscope equipped with an AUTOSCAN™ stage. The ages were calculated using the TRACK KEY program, version 4.2.f (Dunkl 2002). Thermal histories of the samples were modelled using the HeFTy® modelling program, version 1.6.7 (Ketcham 2005) and the annealing model of Ketcham et al. (2007).

4 Magmatic characterisation and U/Pb ages of the BVS

4.1 Petrography and chemistry

The investigated rocks include mainly samples from cores of volcanic pebbles (up to some dm in diameter) from epiclastic rocks (Fig. 2) and few samples of massive lava flows. These lavas reveal a porphyritic to glomeroporphyritic texture defined by several mm-sized phenocrysts embedded into a micro granular matrix (Callegari et al.

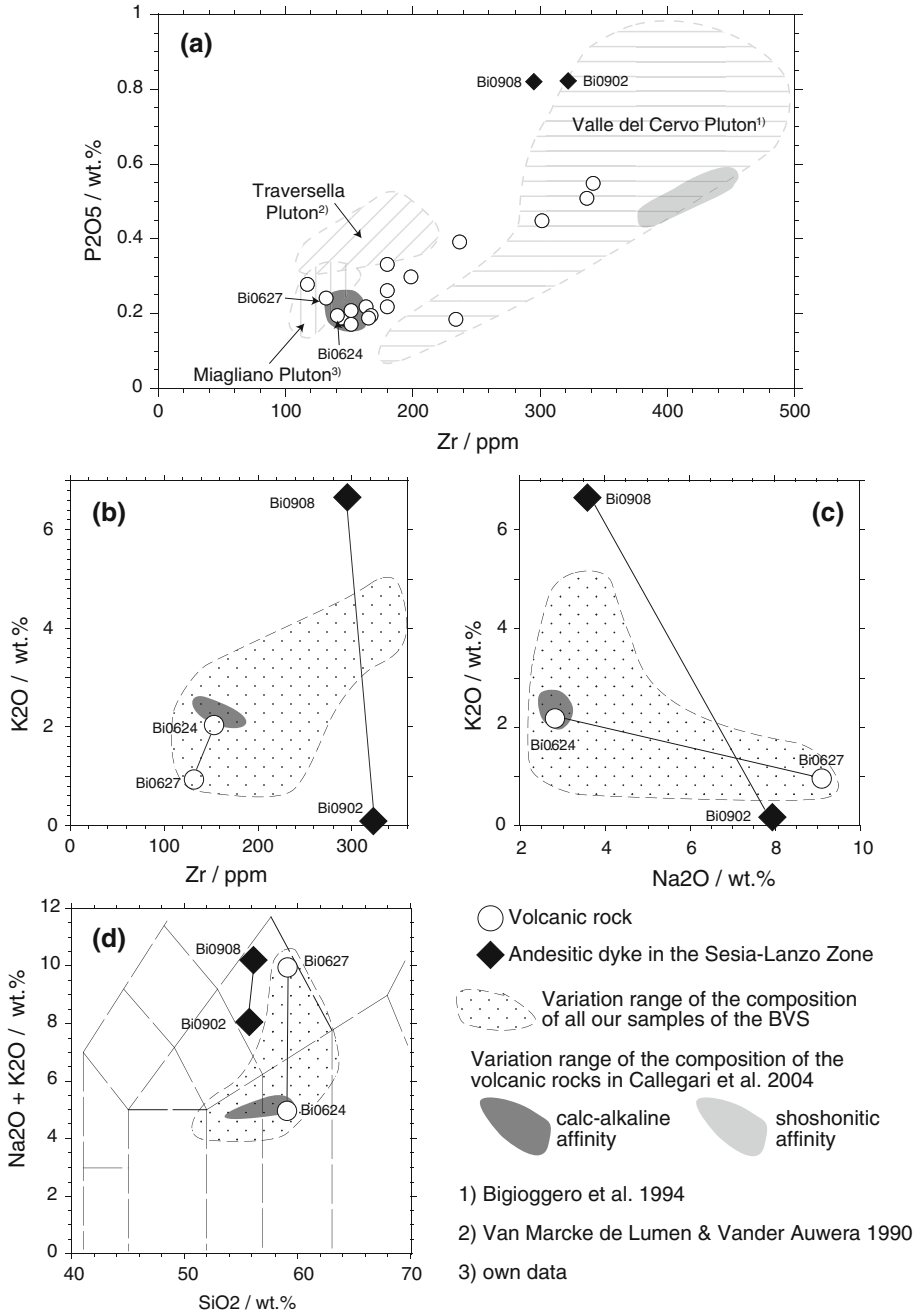

Fig. 3 Bulk chemical analyses of the rocks of the BVS, volcanic dykes and Miagliano Pluton compared with data of Callegari et al. (2004) and data of the Valle del Cervo Pluton (Bigioggero et al. 1994) and Traversella Pluton (Van Marcke de Lumen and Vander Auwera 1990). **a** Zr–P_2O_5 diagram showing the distribution of our samples of volcanic rocks in relation with the data of Callegari et al. (2004) and with the data from the plutonic rocks (Valle del Cervo Pluton, Miagliano Pluton and Traversella Pluton). **b** Zr–K_2O plot illustrating the strong effect of alteration on K_2O by nearly unchanged Zr concentration. **c** Na_2O–K_2O plot showing contrasting enrichment/depletion behaviour of samples with similar primary composition. **d** Total alkali silica (TAS) diagram illustrating the effect of antithetic enrichments on the nomenclature of volcanic rocks

2004). The idiomorphic to xenomorphic phenocrysts are plagioclase, orthopyroxene, clinopyroxene, amphibole and biotite. Sanidine occurs only in few samples belonging to the shoshonitic series. The matrix consists of plagioclase, pyroxene, amphibole, biotite and newly developed phases (see next section). The groundmass surrounding the well-rounded components of the epiclastic rocks consists of a fine-grained breccia of angular mm- to cm-sized volcanic fragments and xenoliths such as phengite and quartz grains derived from the Sesia–Lanzo zone.

Callegari et al. (2004) have presented an exhaustive geochemical treatment of the volcanic rocks finalized to the description of their magmatic evolution and we will compare our results mainly with this data set. Other more general contributions on the characterisation of the geochemical signature of the Oligocene magmatism in the Sesia–Lanzo zone have been published (Dal Piaz et al. 1979; De Capitani et al. 1979; Beccaluva et al. 1983; Venturelli et al. 1984; Owen 2008; Conticelli et al. 2009). We have analyzed only samples that have been used for the description of the alteration and dating, in order to reproduce the subdivision in calc-alkaline and shoshonitic proposed by Callegari et al. (2004). Consequently our data are strongly influenced by the redistribution of the all

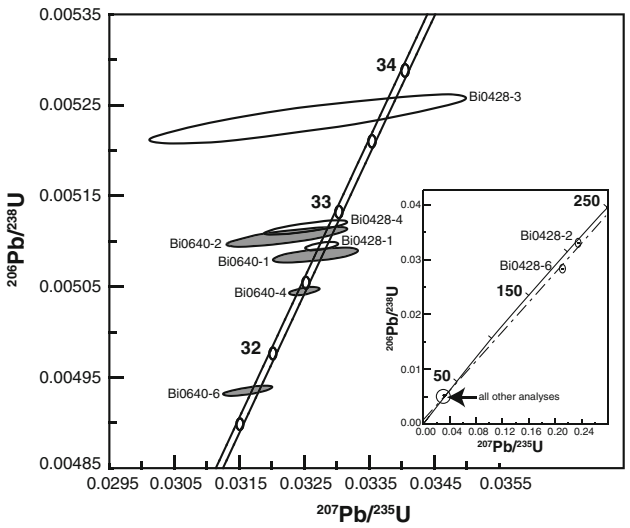

Fig. 4 Concordia diagram showing the results of U–Pb age determination for the rocks of the BVS (see Table 1). Inset shows the two samples with inherited component of Paleozoic age

elements sensitive to some kind of alteration processes and cannot be used in classification schemes. However, some elements less affected by hydrothermal alteration (e.g., Zr, P) have been utilized to compare our samples with the published data (Van Marcke de Lumen and Vander Auwera 1990; Bigioggero et al. 1994; Callegari et al. 2004; Fig. 3a). The effects of the different stages of alteration are well illustrated using the mobile alkaline elements (Fig. 3b–d). Figure 3b supports the assumption that even strong alteration does not affects significantly the concentration of Zr and justifies the use of this element in comparative diagrams (Fig. 3a). Two andesitic dykes crosscutting the Sesia–Lanzo zone in the upper Val Sessera belonging to the same shoshonitic series and with a similar primary composition (Fig. 3a), but they show a completely different K_2O–Na_2O exchange behaviour (Fig. 3c). Sample Bi0908 is enriched in K_2O at nearly constant Na_2O content, whereas sample Bi0902 is completely depleted in K_2O, but massively enriched in Na_2O. Such differences show the changes of the alteration conditions (e.g., P, T, fluid composition, fluid/rock ratio). Similarly, sample Bi0627 is slightly depleted in K_2O and strongly enriched in Na_2O in respect to sample Bi0624 from the same lava flow some few metres distant of Bi0627 (Fig. 3c). Beside the effects due to the different types of alteration, this suggests also a strong localisation of these processes leading to an extremely complex patchwork like distribution of the chemical compositions. In the case of singular enrichment (e.g., K_2O in Bi0627), the differences between the two samples simply increases and leads to a different rock name, but, in case of antithetic exchanges of K_2O and Na_2O as in Bi0902 and 0908, potential primary differences between the samples could have been reduced. Owing all these difficulties, the comparison with the data of Callegari et al. (2004) clearly indicates that the majority of our samples are andesitic in composition with calc-alkaline affinity. Only few samples show a clear enrichment of Zr at similar andesitic composition suggesting a shoshonitic affinity.

4.2 U/Pb dating

Scheuring et al. (1974) have determined an age range between 29 and 33 Ma for the BVS by K/Ar methods. Zingg et al. (1976) pointed out that these ages may have been influenced by a reheating event and dated the age of this low temperature metamorphism at around 31 Ma by means of a K/Ar age of illite in a tuffite layer of the BVS. We decided to date single grain zircon crystals, which should be less affected by such low temperature alteration. However, in the case of the BVS also the potential incorporation of inherited zircon xenocrysts in the magma may introduce complication during single grain dating. This is of special importance, because of the time overlap of the Alpine metamorphism in the Sesia zone and the emplacement of BVS magmas. In order to address this topic, we have inspected the zircons grains using cathodoluminescence and BSE methods. Most grains show concentric zonations, but also patchy types exist. These zonations are typical for magmatic zircons. The dated sample Bi0428 belongs to a massive andesitic lava flow at Bocchetta di Sessera. Three out of five zircon crystals from this sample are concordant within error, and yield $^{206}Pb/^{238}U$ dates between 32.74 and 33.66 Ma (Fig. 4). Analyses Bi0428-2 and Bi0428-6 are discordant and have Paleozoic upper intercepts (Table 1). Sample Bi0640 is a rounded calc-alkaline andesitic component within the epiclastic conglomerate of the BVS in Val Oropa. All four zircon crystals from this sample define concordant $^{206}Pb/^{238}U$ dates from 31.62 to 32.64 Ma, partly overlapping with the observed age range in the previous sample (Fig. 4; Table 1). Following the arguments of Furrer et al. (2008) and Schaltegger et al. (2009), the magmatic zircon crystallises during cooling and fractionation in the calc-alkaline series. This is consistent with the typical magmatic zoning pattern described above. Therefore, we assume that the zircon crystallisation age approximates that of the volcanic eruption. Most ages spread between 32.44 and 32.89 Ma, possibly reflecting magma chamber processes (e.g., Schaltegger et al. 2009; Simon et al. 2008). Zircon Bi0428-3, containing high common lead concentrations (95 % of the total lead), may contain a small inherited core. Zircon Bi0640-6 is younger than the main group of ages, this may be caused by local, minor Pb loss, not being completely

Table 1 Isotope data of single grain zircon analysis

Number[a]		Concentrations				Atomic ratios								Apparent ages		
	Weight (mg)	U	Pb total (ppm)	Pb nonradiation (pg)	Th/U[b]	206/204[c]	207/206[d, e]	Error 2 s (%)	207/235[d, e]	Error 2 s (%)	206/238[d]	Error 2 s (%)	Correction	206/238[e]	207/235	207/206[e]
Bi0428																
0428-1	0.0082	161	0.87	0.66	0.52	657	0.04665	0.59	0.03277	0.63	0.00509	0.07	0.58	32.76	32.74	31.39
0428-2	0.0043	233	7.75	0.94	0.28	2,235	0.05165	0.17	0.23489	0.19	0.03299	0.06	0.47	209.21	214.21	269.94
0428-3	0.0040	49	0.27	1.04	0.55	92	0.04510	5.75	0.03255	6.12	0.00523	0.43	0.87	33.66	32.52	−50.20
0428-4	0.0044	409	2.16	2.16	0.46	284	0.04611	1.51	0.03252	1.61	0.00511	0.13	0.80	32.89	32.49	3.35
0428-6	0.0034	53	1.47	0.57	0.19	584	0.05411	0.50	0.21118	0.55	0.02831	0.09	0.58	179.94	194.54	375.63
Bi0640																
0640-1	0.0083	118	0.63	0.95	0.52	345	0.04659	1.52	0.03266	1.60	0.00508	0.13	0.64	32.69	32.64	28.30
0640-2	0.0058	66	0.35	0.61	0.48	219	0.04580	2.23	0.03224	2.37	0.00510	0.18	0.80	32.82	32.21	−12.89
0640-4	0.0021	853	4.42	0.79	0.43	733	0.04674	0.55	0.03251	0.58	0.00505	0.07	0.55	32.44	32.48	35.97
0640-6	0.0041	2,197	12.77	13.33	0.42	229	0.04648	0.91	0.03163	0.97	0.00494	0.09	0.74	31.74	31.62	22.58

[a] All zircons annealed-leached, all single grains

[b] Calculated on the basis of radiogenic Pb^{208}/Pb^{206} ratios, assuming concordancy

[c] Corrected for fractionation and spike

[d] Corrected for fractionation, spike, blank and common lead (Stacey and Kramers 1975)

[e] Corrected for initial Th disequilibrium, using an estimated Th/U ratio of four for the melt

Table 2 Intensity and distribution of the alteration

	Valle dell'Elvo	Val Oropa	Valle del Cervo	Bocchetta di Sessera	Val Sessera
Calcite	x	xxx	xxx	xx	x
Chlorite	x	xx	xx	x	x
Quartz	x	xx	xx	x	x
Clay minerals	x	xx	xx	x	x
Hematite/lepidocrocite	xx	x	x	x	x
Zeolite	x	x	x		
Pumpellyite	x				
Serpentine	x				

[x] Observed
[xx] Frequent
[xxx] Dominant

removed by the chemical abrasion pre-treatment. The remnant five ages (Bi0428-1, 4 and Bi0640-1, 2, 4) indicate zircon crystallization within a time frame of 450 ka (32.44–32.89 Ma). This is the best estimate for zircon crystallization and eruption of the BVS.

5 Metamorphic evolution

The BVS displays widespread post-emplacement mineralogical transformations. In order to unravel this alteration, several processes have to be considered. (1) Influence of fluids, gases and heat during the volcanic activity, (2) alteration at the paleosurface, (3) sub-surface very low-grade metamorphic re-crystallisation or authigenic crystallisation during tectonic movements, (4) metamorphism related to the residence of the sequence at uppermost crustal levels during the Neogene, and (5) finally, it cannot always be excluded that some alteration may have been formed during the recent re-exposition at the surface.

The type and intensity of alteration differ at the outcrop scale, but also between the different outcrops (Table 2). Whereas the rocks of the BVS at Sordevolo are slightly altered, the rocks further north reveal a stronger alteration mainly characterized by the occurrence of calcite, chlorite, clay minerals and quartz. We distinguished between phenocrysts alteration, matrix alteration and phases formed in amygdules or veins. In all volcanic rocks of the studied area, orthopyroxene is completely replaced by chlorite (Fig. 5a). Clinopyroxene is either fresh or altered to calcite. Calcite and clay minerals are the typical alteration products of plagioclase. In the northern most part, plagioclase is partially overgrown by chlorite (Fig. 5a). Cavities within the matrix are partially filled with newly developed phases such as calcite, chlorite, clay minerals, hematite, lepidocrocite and authigenic quartz (Table 3; Fig. 5b, c). The newly developed phases within the matrix normally do not exceed the clay grain size. One example (Val Oropa) shows irregularly shaped amygdules within the matrix of the conglomerates, which contain complex infillings of several alteration minerals. The sequence of multi-phase fillings, for example the micro-granular quartz followed by chlorite and finally sparry calcite (Fig. 5b), can be interpreted as consequence of changing saturation conditions in the fluid. Other amygdules have thin rims of quartz and clay minerals and fibrous quartz in the centre. In addition, dispersed hematite and lepidocrocite occur within the matrix bounding the individual components of the conglomerates (Fig. 5c). These phases show complex grow structures (alternation of micro-layers of different colours) indicating a multi-stage development. A dark red layer seems to represent earlier infiltrations, whereas later fillings are lighter red and often associated with chlorite. Zeolite, pumpellyite and serpentine have been determined by X-ray diffractometry (XRD). Veins are easily distinguished from the above-mentioned amygdule as they crosscut discordantly the whole rock (clasts as well as matrix of the conglomerates) and have definite boundaries. Nearly all veins contain carbonates and/or quartz and are restricted to the area of Val Oropa and Valle del Cervo (Table 3).

The crystallinity of illite and chlorite was determined by XRD. The results indicate the coexistence of different phases within a drilled volume of each sample, as a mixture of different generations or textural types cannot be avoided using this method. Measurements on air-dried and ethylene–glycol-solvated samples indicate a lack of inter layers of smectite and vermiculite. Figure 6 shows the full width at half maximum (FWHM) of the illite 10 Å peak (Ill002) versus the FWHM of the chlorite 14 Å peak (Chl001) of the BVS. Kübler (1967) used FWHM determinations of the illite 10 Å peak to distinguish three zones with increasing metamorphic grade (diagenetic zone, anchizone and epizone). The anchizone in the Alps (with FWHM of the illite 10 Å peak between 0.25 and 0.42°2θ) corresponds approximately to the temperature range between 200 and 300 °C (Frey 1986). Arkai (1991) defined the anchizone with FWHM of the chlorite 14 Å peak between 0.31 and 0.43°2θ. The FWHM of the illite 10 Å peak of the rocks of the BVS ranges between 0.10 and 0.75°2θ, and the FWHM of the chlorite 14 Å peak between 0.27 and 0.62°2θ.

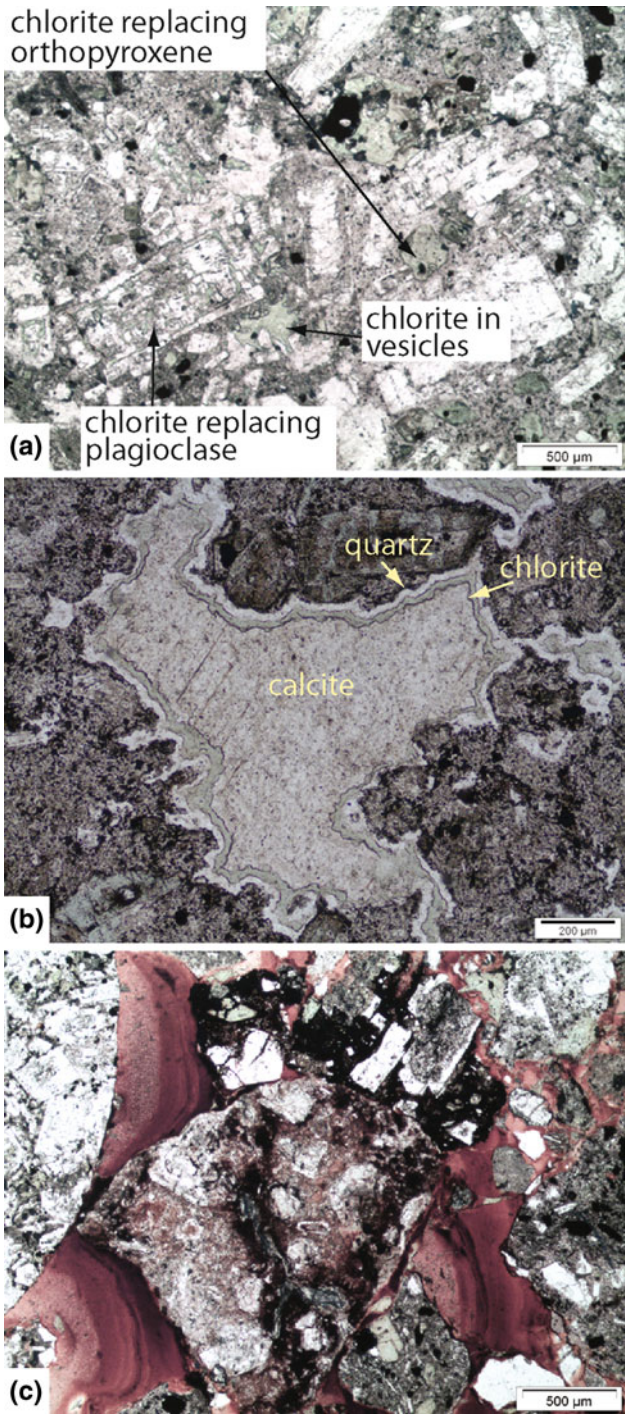

Fig. 5 Thin section photographs, plane polarised light: **a** chlorite replacing orthopyroxene and plagioclase as well as filling pore space in the matrix; **b** amygdule filled with calcite and rimmed by chlorite and quartz (Valle, Val Oropa); **c** pore space in the matrix of the conglomerates filled with hematite and lepidocrocite. The early infiltrations are represented by *dark red* lamellae; later fillings are *lighter red*

The XRD analyses plot in the fields of the anchizone and diagenetic zone and refer to temperatures less than 300 °C (Fig. 6).

6 Fission track data

Apatite fission track data are available for the samples Bi0704 and Bi0706, and zircon fission track data for the samples Bi0704, Bi0706, Bi0701 and Bi0710 (Fig. 7). Sample Bi0706 belongs to a massive andesitic lava flow at Bocchetta di Sessera; the other samples are from rounded volcanic components within the epiclastic conglomerate of the BVS in Sordevolo (Valle dell'Elvo), Valle (Val Oropa) and Passobreve (Valle del Cervo). The fission track ages indicate no correlation with sampling altitude. Both apatite specimens pass the χ^2 test (χ^2 (%) > 5) with no indication of subpopulations (Table 4). Calculated central ages for these samples are thus interpreted to represent cooling ages. Apatite fission track ages are 20.3 ± 2.8 Ma and 15.5 ± 2.3 Ma for sample Bi0704 and Bi0706, respectively. Zircon fission track central ages are 17.3 ± 2.0 Ma for sample Bi0710 and 24.2 ± 1.9 Ma for sample Bi0706 (Table 5). The two other zircon specimens (Bi0701 and Bi0704) fail the χ^2 test (Table 5).

Apatite and zircon fission track ages are more than 10 million years younger than the age of the sub-aerial emplacement of this rock (32.65 Ma) and refer to subsequent annealing of the fission tracks after burial of the BVS. This problem has been additionally modelled using HeFTy® software and the FT input data of sample Bi0704 and Bi0706 (Fig. 8). The eruption of the rocks of the BVS at the surface around 33 Ma (initial t–T box) was used as start point for the modelling of the fission track data. The second t–T box was defined by the zircon age of the respective sample within the zircon partial annealing zone temperature range (180–300 °C). The modelled t–T paths of both samples are very similar and clearly indicate post-depositional reheating. This was followed by enhanced cooling of the samples to the upper limit of the apatite partial annealing zone in the early Miocene, a subsequent prolonged residence of the samples within the apatite partial annealing zone from about 20 to 5 Ma and a final increase in cooling (Fig. 8).

7 Discussion

7.1 Magmatism and its time relations

The formation of the BVS can be associated with sub-aerial effusive and explosive volcanic activity as well as the products of their epiclastic reworking (Callegari et al. 2004). The characteristics of the epiclastic rocks (see Sect. 2) indicate relatively immature sediment textures and compositions, the absence of marine indicators, in particular fossils, and channel geometries allow to classify these rocks as alluvial sediments (Reading 1996). Normally, an

Table 3 Main alteration minerals

	Alteration primary minerals south	Alteration primary minerals north	Void infillings south	Void infillings north	Veins in Val Oropa	Veins in Valle del Cervo	Veins in Val Sessera
Calcite	xxx	xx	x	x	xxx	xxx	x
Chlorite	xxx	x	x	x			
Quartz			x	x	xx	xx	x
Clay minerals	xxx	xxx	x	x			
Hematite/lepidocrocite	x	x	x	x			
Zeolite			x	x			
Pumpellyite			x				
Serpentine			x				
Ankerite					xxx	xxx	
Tourmaline						xxx	
Barite					x		

[x] Observed

[xxx] Frequent

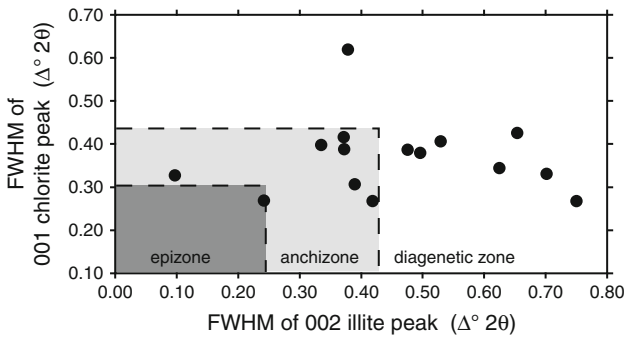

Fig. 6 Relationships between the full width at half maximum (FWHM) of the illite 10 Å peak (Ill002) versus the FWHM of the chlorite 14 Å peak (Chl001) for illite and chlorite occurring within the BVS. Subdivision of zones with increasing metamorphic grade with FWHM of illite according to Kübler (1967) and FWHM of chlorite according to Arkai (1991)

epiclastic layer is the first unit overlaying the regolith on top of the gneisses of the Sesia–Lanzo zone (Kapferer et al. 2011).

Sedimentation in volcanic settings differs significantly from transport and deposition of rocks in other environments. The difference may be attributed to periodic catastrophic volcanic eruptions, which locally produce unvegetated high-relief slopes and allow extremely high local rates of erosion and subsequent fluvial-deltaic sedimentation. The outcrops in the studied area do not provide information regarding the position and geometry of the former volcanic edifices. The following reasons support the assumption that the rocks of the BVS derived from one or more stratovolcano(es): (1) Stratovolcano morphology results from repeated eruptions of pyroclastic and relatively short lava flows; (2) volcaniclastic deposits (pyroclastic and epiclastic) are usually more important volumetrically than effusive deposits; (3) stratovolcanoes are prone to mass-wasting, because they are high topographic features. During periods of eruptive quiescence, normal surface processes such as erosion and sedimentation operate at very high rates; (4) andesitic magmas form typically stratovolcanoes; and (5) stratovolcanoes are frequently polygenetic. Vessel and Davies (1981) studied epiclastic processes of a stratovolcano based on studies of Fuego, Guatemala, and divided its deposits into four facies associations. The volcanic products of the BVS fit well the depositional character of the transition zone between the proximal and medial volcaniclastic facies of the latter study. The massive rocks at Bocchetta di Sessera and in Val Sessera indicate the spatial proximity to the eruptive centre. The fluvial conglomerates with well-rounded components represent the medial volcaniclastic facies.

The timing of the eruption of the volcanic rocks is inferred from the crystallisation age of zircons in a shallow magma chamber at ~ 33–32 Ma (see section on U/Pb dating). The nearby Miagliano tonalite overlaps in age with these zircons and is part of the same calc-alkaline evolution (Berger et al. 2012b). The chemical variations of some of the plutonic, subvolcanic and volcanic rocks indicate calc-alkaline evolution developed in a narrow time interval. This is consistent with the model of Callegari et al. (2004), who proposed AFC processes with a basaltic parental melt. The zircon crystal including a relict old core discussed previously is consistent with such an evolution (Table 2). In contrast, some of the alkaline rocks require a different parental melt (e.g., Owen 2008; Conticelli et al. 2009). In addition, the different members of the Valle del Cervo Pluton can be better explained by simple crystal fractionation from a monzonitic parental melt (Bigioggero et al.

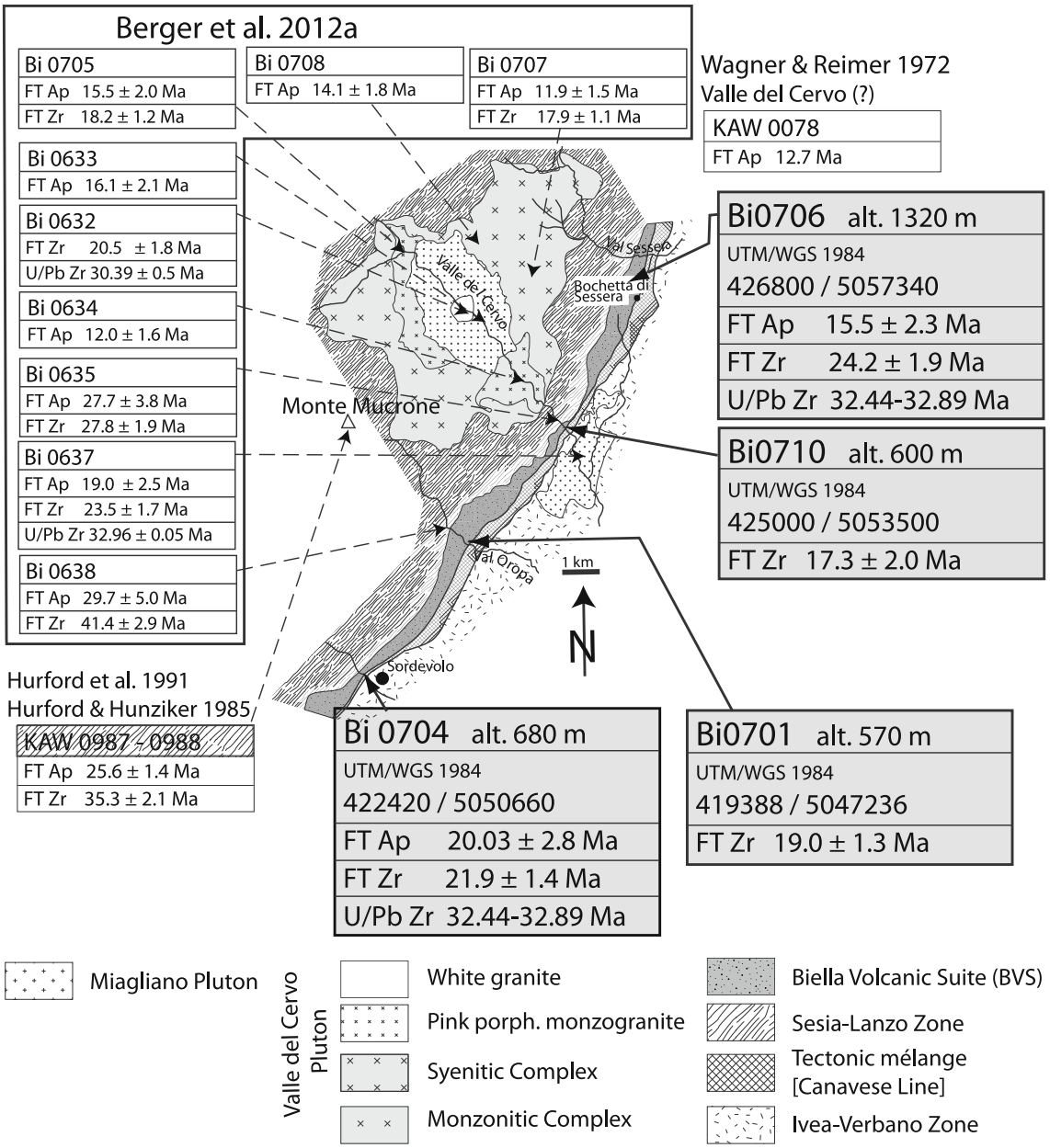

Fig. 7 Geological map of the Biella area (see Fig. 1 for details) with the distribution of the fission track data of this study (*grey shaded boxes*) and from the literature (*white boxes*)

Table 4 Apatite fission track data

Sample	Altitude	Counted grains	N_s	ρ_s (10^5 cm^{-2})	N_i	ρ_i (10^5 cm^{-2})	χ^2	Age ± 1σ (Ma)	Dpar (μm)	Track length ± 1σ (μm)	Tracks measured
Bi0704	680	17	159	4.625	1,837	53.438	99.81	20.3 ± 2.8	2.55	12.7 ± 2.0	39
Bi0706	1,320	16	181	4.778	2,854	75.340	13.36	15.5 ± 2.3	2.24	11.8 ± 1.9	24

N_s number of spontaneous tracks counted on the sample, ρ_s density of spontaneous tracks, N_i number of induced tracks counted on the glimmer detector, ρ_i density of induced tracks, χ^2 result of the statistical test in %, *Dpar* measured long axis of etch pits on the polished surface in μm, *Mean track length* mean length of horizontal confined tracks in μm given with 1σ error

Table 5 Zircon fission track data

Sample	Altitude	Counted grains	N_s	ρ_s (10^5 cm^{-2})	N_i	ρ_i (10^5 cm^{-2})	χ^2	Age $\pm$ 1σ (Ma)
Bi0701	570	20	1,649	46.743	3,982	112.876	0.24	19.0 $\pm$ 1.3
Bi0704	680	20	2,211	45.569	4,612	95.054	0.02	21.9 $\pm$ 1.4
Bi0706	1,320	15	532	19.683	1,025	37.923	30.83	24.2 $\pm$ 1.9
Bi0710	600	10	163	10.929	458	30.708	19.95	17.3 $\pm$ 2.0

N_s number of spontaneous tracks counted on the sample, ρ_s density of spontaneous tracks, N_i number of induced tracks counted on the glimmer detector, ρ_i density of induced tracks, χ^2 result of the statistical χ^2 test in %

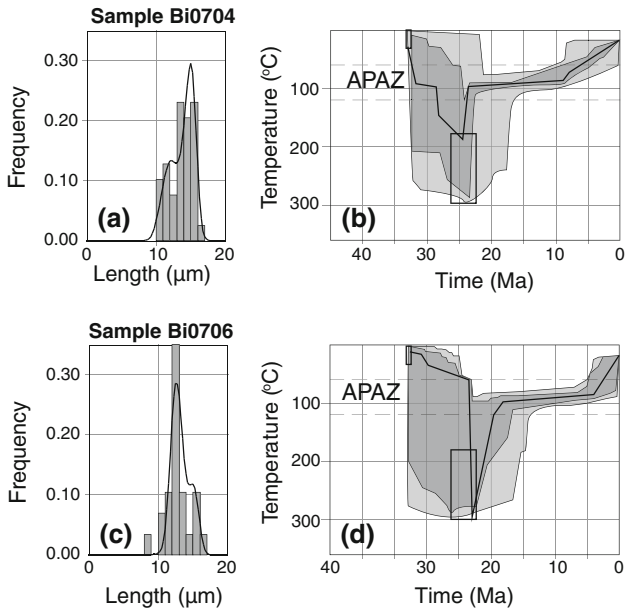

Fig. 8 Modelled time–temperature (t–T) paths of two samples of the rocks of the BVS are presented. The modelling was carried out using the HeFTy® program. The areas classified with "good fit" envelope paths (*dark grey*) have a merit value of 0.05. A merit of 0.5 is required for the "acceptable fit" paths (*light grey*). The thick black line is the modelled "best fit" path. The diagrams on the right show the measured (*bars*) and modelled (line for the best-fit model) track length distribution

1994). This magmatic evolution and the relative timing of emplacement seem to rule out a direct magmatic genetic relationship between the BVS and the Valle del Cervo Pluton (compare Callegari et al. 2004; Berger et al. 2012b).

The volcanism in Biella is coeval and similar in composition as the relicts of volcanic clasts found in the Taveyannaz sandstone formation of the Helvetic Flysch system (Vuagnat 1983; Fischer and Villa 1990; Sinclair 1992; Ruffini et al. 1997). Lacking clear evidence for a proximal source of the volcanic clasts in the Taveyannaz formation, the volcanism in Biella has been suggested as potential candidate (Ruffini et al. 1997; Beltrando et al. 2010). If this is the case, the Rupelian drainage divide in the Western Alps must have been situated in the most internal portion of the growing mountain range, much further south-east than today (see Schlunegger et al. 2001; Spiegel et al. 2001). Finally, the volcanism in Biella is slightly older then the Mortara volcanism (28.5 Ma; Di Giulio et al. 2001; Pieri and Groppi 1981; Ruffini 1995). The petrographic description and the geochemical data of the Mortara volcano (Ruffini 1995) indicate a volcanism similar to the BVS.

The geodynamic context of this Rupelian magmatism is related to the ongoing subduction of Piemonte-Liguria, Briançonnais and European units below the Austroalpine Sesia–Lanzo zone and Ivrea-Verbano zone. The complex geochemical characteristics of this magmatism (Dal Piaz et al. 1979; De Capitani et al. 1979; Beccaluva et al. 1983; Venturelli et al. 1984; Owen 2008; Conticelli et al. 2009; Tommasini et al. 2011) are discussed in Berger et al. (2012b).

7.2 Metamorphism of the BVS

The development of very low-grade mineral assemblages, the occurrence of hydrothermal veins as well as fission track data provide evidence for burial of the BVS with the subjacent rocks of the Sesia–Lanzo zone. Unfortunately, the extremely small grain size of the new metamorphic minerals do not permit a clear chronological differentiation between the different steps of the post-emplacement metamorphic overprint (hydrothermal alteration during the volcanic activity; alteration at the paleosurface; very low-grade metamorphic re-crystallisation and authigenic crystallisation during tectonic movements; recent surface exposition). However, some important general limits can be inferred: (1) neither epidote nor actinolite, possible indicators of higher metamorphic temperatures, has been found by SEM or XRD methods (Fig. 9); (2) crystallinity data show a large spread, but the best ordered sheet silicates, which are newly developed (growing in voids), indicate conditions related to burial (see discussion below); (3) zeolite minerals are stable phases; (4) the rejuvenation of the zircon FT age imposes a reheating up to 250 °C.

Petrogenetic grids for basaltic and andesitic composition show reactions forming clinozoisite/epidote at 200 and 300 °C, depending on X_{CO_2} (Fig. 9; Frey et al. 1991; Digel and Ghent 1994). The absence of actinolite and epidote indicates that these conditions were not reached. Similar

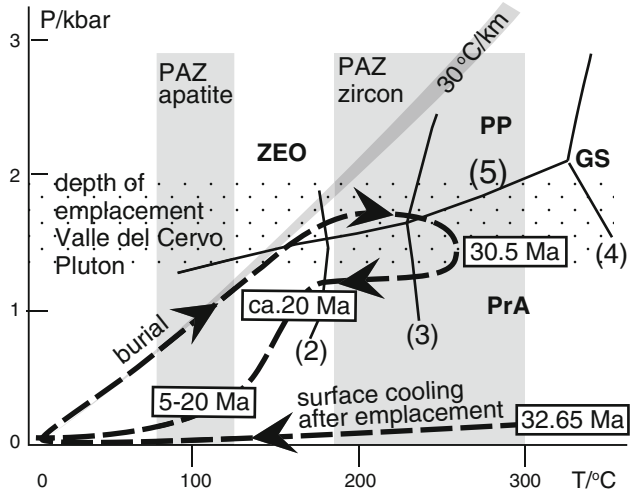

Fig. 9 P–T diagram for basaltic systems redrawn from Robinson and Bevins (1999) with the suggested PTt path for the BVS. The petrogenetic grid is determined for NCMASH system modified after Liou et al. (1987); see also Frey et al. (1991) 1: Prh + Chl + Lmt = Pmp + Qtz + H_2O; 2: Arn + Qtz = Ab + H_2O; 3: Lmt + Prh = Cz + Qtz; 4: Prh + Chl + Qtz = Cz + Tr + H_2O; 5: Pmp + Qtz = Cz + Prh + Chl + H_2O. *ZEO* zeolite facies, *PrA* prehnite-actinolite facies, *PP* prehnite-pumpellyite facies, *GS* greenschist facies. Partial annealing zone for zircon and apatite as well as the emplacement depth of the Valle del Cervo Pluton are indicated

conclusion can be inferred from the crystallinity data on sheet silicates. The spread in the data reflects the entire spectrum of clay and chlorite formation during the different stages of alteration, from the paleosurface through the burial until the final exhumation. However, the FWHM estimations of illite and coexisting chlorite, confirm the burial of the BVS as they clearly indicate temperatures higher than those expected at the surface. The FWHM data of the best ordered clay and chlorite reach only temperature conditions at the transition between the anchizone and the epizone (Fig. 7). Finally, crystallinity data, mineral occurrence and FT data agree with a post-emplacement burial of the volcanic rocks but exclude conditions higher than those of the prehnite-pumpellyite facies for the metamorphic overprint of the main part of the BVS. Zingg et al. (1976) used whole rock samples and only the fraction below 2 μm, but without the textural selection used in this study. Even if the data may not be directly comparable, the crystallinity data of their study also indicate mainly anchizone/diagenesis condition (Zingg et al. 1976). These authors interpreted their data as re-heating of the volcaniclastic rocks by overriding hot andesite flows. However, except at Bocchetta di Sessera, essentially epiclastic rocks of the BVS cover the rocks of the Sesia–Lanzo zone and the regolith. These polymictic conglomerates, containing well-rounded components of volcanic origin and of rocks of the Sesia–Lanzo zone, refer to an alluvial depositional environment. Therefore, a thermal input directly from these rocks can be excluded. The increase in temperature of the epiclastic rocks of the BVS must be related to the burial of the whole stratigraphic sequence (i.e., the gneisses of the Sesia–Lanzo zone, the regolith on top of them and the BVS). Despite of equilibration problems, the combination of identified minerals and crystallinity data make conditions at the border between the zeolite and the prehnite-pumpellyite facies most likely (Fig. 9). The identified zeolite may not reflect the maximum temperatures. A thermal overprint can be confirmed by the FT ages, which are distinctly younger than the eruption age of the volcanic rocks. The zircon fission track ages (17–24 Ma) are 10–15 Ma younger than the crystallisation age (~33 Ma). In spite of the large variation in zircon single grain ages and the variations of central ages between the samples, indicating an incomplete resetting of the FT during this metamorphic event, the burial of these rocks inside the partial annealing zone of the zircons is certain. This conclusion is confirmed by similar FT age relationships for the Valle del Cervo Pluton and Miagliano Pluton. Both show zircon FT ages 10 Ma younger than the intrusion ages (Berger et al. 2012b). Consequently, the plutons and the BVS remained below or within the partial annealing zone of zircon during Chattian and Aquitanian. In the Burdigalian this crustal block is exhumed in the partial annealing zone of apatite where it remains the entire Miocene. It is difficult to relate directly the FT data of the Biella area with literature data from other portion of the Sesia–Lanzo zone due to the Oligocene–Miocene fragmentation of this unit in small domains with slightly different exhumation history (Hurford and Hunziker 1985; Hurford et al. 1991; Malusá et al. 2005, 2006; Berger et al. 2012a). Berger et al. (2012a) describe the individualisation of such block during exhumation of the internal domain of the Western Alps. In particular, they discuss rigid block rotation of the Sesia–Lanzo zone including the BVS and the related burial (see also Fig. 11 in Berger et al. 2012b).

The mutual relationships between BVS and Valle del Cervo Pluton offer the possibility to evaluate the depth of burial of the BVS and therefore to extrapolate a local geothermal gradient as well as heating and burial rates. Especially in the section along the Valle del Cervo, a network of sub-vertical veins affects the rocks of the BVS. Bernardelli et al. (2000) have shown a clear continuity of these veins from the BVS, across the subjacent gneisses of the Sesia–Lanzo zone until the margin of the Valle del Cervo Pluton. These authors interpret the veins as the product of the hydrothermal circulation related to the emplacement of the pluton and suggest temperatures lower than 450 °C for the vein forming fluids. Bernardelli et al. (2000) suggest a very shallow intrusion depth, 2 km, for the Valle del Cervo Pluton in the region of Passobreve. They calculate this depth from the difference between a

pressure of 0.2–0.25 GPa at the base of the intrusion (its NW end) and its nowadays exposed diameter (6.5 km), assuming a post-intrusion rotation of the pluton. The idea of the rotation of the internal part of the Sesia–Lanzo zone was proposed by Lanza (1977, 1979) on the base of paleomagnetic data on the andesitic dykes and andesitic lavas. Bernardelli et al. (2000) consider the asymmetrical distribution of the syn-intrusive hydrothermal mineralization (concentrated along the SW margin of the pluton) and of the intensity of the contact metamorphism as indication of post-intrusive rotation of the pluton. After the detailed analysis of the contact aureole of Zanoni et al. (2010) no clear asymmetry results in the distribution of the P/T data and the pressure seems to be constant at 0.2 GPa all around the pluton. Furthermore, Hrouda and Lanza (1989) have described the orientation of the magnetic lineation and foliation in the Valle del Cervo Pluton as typical for the roof of an intrusion and unaffected from significant post-emplacement tectonic movements. Finally, the nearly concentric cartographic expression of different members of the Valle del Cervo Pluton (Fig. 1; Bigioggero et al. 1994) in combination with deep valley incisions (up to 1,000 m elevation difference) clearly indicate vertical contacts within the pluton and towards the country rocks. We conclude therefore, that the rotation of this portion of Sesia–Lanzo zone predates the intrusion of the Valle del Cervo Pluton and affects only the BVS and its substrate. Consequently, the present day geometry of the pluton can be considered as the original one (see profile in Fig. 1). This is also in agreement with the observations of Bigioggero et al. (1994) describing the emplacement structures of the pluton as the result of "cauldron subsidence". Based on petrologic barometers ("Al-in Hbl" and mineral paragenesis in the contact aureole) crystallisation depths around 5–6 km has been calculated (Bigioggero et al. 1994; Bernardelli et al. 2000; Zanoni et al. 2008, 2010).

In absence of any important tectonic structure able to reduce sensibly the distance between the pluton and the BVS, the present day distance between BVS and pluton (ca. 700 m) must be assumed as the original distance at the moment of the intrusion. It results that the BVS was buried at depth around 5 km before the intrusion of the pluton. If one assumes 250 °C as central temperature of the zircon partial annealing zone, the local near surface Rupelian geothermal gradient could have reached 50 °C/km. Using 180 °C as upper temperature limit of the partial annealing zone, the gradient can be reduced to 35 °C/km. As the maximum age difference between BVS and pluton is 2 Ma, the resulting burial rate would be around 2.5 km/Ma and a heating rate of 90 or 125 °C/Ma, respectively. The high Rupelian geothermal gradients in the area may be related to the localized advective heat transport caused by the uprising magmas. The rapid burial of the Rupelian paleosurface was governed by rigid block rotation as proposed by Berger et al. (2012a). Thermal relaxation at the end of the magmatic input led to lower, more stable thermal gradients in the Chattian. In Burdigalian times the BVS reached the apatite PAZ whereas the final re-exhumation to the surface started during the Messinian.

8 Summary and conclusion

The BVS is a lower Oligocene volcano-sedimentary unit emplaced on top of the high-metamorphic rocks of the Sesia–Lanzo zone (Mombarone nappe) along the Canavese line. The preserved stratigraphic relationships of the BVS and the rocks of the Sesia–Lanzo zone allow a detailed description of the final stage of the exhumation of this innermost part of the Sesia–Lanzo zone. We can summarize this evolution as follows:

1. Calc-alkaline and shoshonitic lavas extruded sub-aerially in the lower Oligocene (Rupelian). High precision U–Pb zircon dates range at 32.44–32.89 Ma for the emplacement of the volcanic rocks. This age represent also the minimum age for a first exhumation to the surface of the high metamorphic rocks of the Sesia–Lanzo zone.
2. Steep stratovolcanoes were responsible for episodic eruptions of pyroclastic and lava flows. High-energy river systems eroded the volcanic edifices and the subjacent rocks of the Sesia–Lanzo zone accumulating large volumes of epiclastic rocks.
3. This volcanism is coeval to volcanic clasts in the Taveyannaz sandstone formation of the North Helvetic Flysch. It is also coeval with the Mortara volcano buried below the sediments in the Po plain. If the source of the Taveyannaz formation is the location of the BVS, the Rupelian drainage divide in the Western Alps must have been situated in the most internal portion of the growing mountain range.
4. The rocks of the BVS show different types of post-emplacement mineralogical overprint, i.e., surface alteration, very low grade metamorphism and cross-cutting hydrothermal veins partly related to the contact aureole of the Valle del Cervo Pluton. The maximum temperature of this overprint has never exceeded ~250 °C as demonstrated by: (1) newly formed paragenesis with illite, chlorite, pumpellyite, hematite, lepidocrocite, different types of carbonates and quartz; (2) illite/chlorite crystallinity; and (3) the partially annealed FT in zircon.
5. The burial of the BVS predates the intrusion of the Valle del Cervo Pluton. Therefore the depth of burial can be estimated in relationships with the intrusion at

around 5 km (Zanoni et al. 2008, 2010) as the present day minimal distance between BVS and pluton is of only 700 m in Valle del Cervo.

6. The post-emplacement burial at depth around 5 km of the BVS is achieved by near surface rigid block rotation in agreement with the present day geometry (60° dip of the original volcano-sedimentary structures) and the paleomagnetic data of Lanza (1979).
7. The main part of the tilting must take place in time interval between the extrusion of the volcanic rocks (32.44–32.89 Ma) and the intrusion of the Valle del Cervo Pluton (30.5 Ma; Romer et al. 1996; Berger et al. 2012b).
8. The preservation of a paleosurface in polymetamorphic terrains is an exceptional feature and allows the precise reconstruction of its subsequent evolution. In the studied area, the intact Rupelian stratigraphic relationships between the rocks of BVS and of the Mombarone nappe are preserved without important subsequent tectonic reworking. This allows connecting directly the post Eocene evolution of this portion of the Sesia–Lanzo zone with that of the BVS.
9. After Rupelian burial, the BVS and the related portion of the Mombarone nappe remain below the apatite PAZ and are uplifted into the apatite PAZ in the Aquitanian. During nearly the whole Miocene the block remains at that depth until finally, in Messinian times, it started to be exhumed to the surface.

Acknowledgments A Swiss National Research Foundation grants no. 200020-124331 supported this work and the operation of the radiogenic isotope laboratory at University of Geneva. P. Rossetti and an anonymous reviewer are thanked for detailed and careful reviews.

References

Ahrendt, H. (1969). Tertiärer Vulkanismus in der Canavese-Zone? *Neues Jahrbuch für Geologie und Paläontologie, Mitteilungen, 9*, 513–516.

Ahrendt, H. (1972). Zur Stratigraphie, Petrographie und zum tektonischen Aufbau der Canavese-zone und ihrer Lage zur Insubrischen Linie zwischen Biella und Cuorgné. *Göttinger Arbeiten für Geologie und Paläontologie, 11*, 1–89.

Ahrendt, H. (1980). Die Bedeutung der Insubrischen Linie für den tektonischen Bau der Alpen. *Neues Jahrbuch für Geologie und Paläontologie Abhandlungen, 160*, 336–362.

Arkai, P. (1991). Chlorite crystallinity: An empirical approach and correlation with illite crystallinity, coal rank and mineral facies as exemplified by Palaeozoic and Mesozoic rocks of northeast Hungary. *Journal of Metamorphic Geology, 9*, 723–734.

Babist, J., Handy, M.R., Konrad-Schmolke, M. & Hammerschmidt, K. (2006). Pre-collisional, multistage exhumation of subducted continental crust: The Sesia Zone, western Alps. *Tectonics*, *25*, TC6008.

Beccaluva, L., Bigioggero, B., Chiesa, S., Colombo, A., Fanti, G., Gatto, G., et al. (1983). Post-collisional orogenic dyke magmatism in the Alps. *Memorie della Società Geologica Italiana, 26*, 341–360.

Beltrando, M., Lister, G. S., Rosenbaum, G., Richards, S., & Forster, M. A. (2010). Recognizing episodic lithospheric thinning along a convergent plate margin: The example of the Early Oligocene Alps. *Earth-Science Reviews, 103*, 81–98.

Berger, A., Mercolli, I., Kapferer, N., & Fügenschuh, B. (2012a). Single and double exhumation of fault blocks in the internal Sesia-Lanzo Zone and the Ivrea-Verbano zone (Biella, Italy). *International Journal of Earth Science,*. doi:10.1007/s00531-012-0755-6.

Berger, A., Thomsen, T.B., Ovtcharova, M., Kapferer, N., & Mercolli, I. (2012b) Dating emplacement and evolution of the orogenic magmatism in the internal Western Alps: 1. The Miagliano Pluton. *Swiss Journal of Geoscience*, *105*. doi: 10.1007/s00015-012-0091-7.

Bernardelli, P., Castelli, D., & Rossetti, P. (2000). Tourmaline-rich ore-bearing hydrothermal system of lower Valle del Cervo (Western Alps, Italy): Field relationships and petrology. *Schweizerische Mineralogische Petrographische Mitteilungen, 80*, 257–277.

Bianchi, A., & Dal Piaz, G. B. (1963). Gli inclusi di "micascisti eclogitici" della Zona Sesia nella formazione porfiritica permiana della Zona del Canavese fra Biella ed Oropa: Caratteristiche ed età dei fenomeni metamorfici. *Giornale di Geologia, 31*, 39–76.

Bigioggero, B., Colombo, A., Del Moro, A., Gregnanin, A., Macera, P., & Tunesi, A. (1994). The Oligocene Valle del Cervo Pluton: An example of shoshonitic magmatism in the Western Italien Alps. *Memorie della Società Geologica Italiana, 46*, 409–421.

Biino, G., & Compagnoni, R. (1989). The Canavese Zone between the Serra d'Ivrea and the Dora Baltea River (Western Alps). *Eclogae Geologicae Helvetica, 82*, 413–427.

Bowring J.F., McLean. N.M. & Bowring S.A., (2011). Engineering cyber infrastructure for U–Pb geochronology: Tripoli and U–Pb Redux. *Geochemistry Geophysics Geosystems, 12*, Q0AA19.

Callegari, E., Cigolini, C., Medeot, O., & D'Antonio, M. (2004). Petrogenesis of calcalkaline and shoshonitic post-collisional Oligocene volcanics of the Cover Series of the Sesia Zone, Western Italien Alps. *Geodinamica Acta, 17*, 1–29.

Carraro, F. (1966). Scoperta di una serie carbonifera di coperture degli Gneiss-Sesia. *Bollotino della Societa Geologica Italiania, 85*, 241–252.

Caviezel, A. (2007). *Hydrothermal veins related to the Valle del Cervo pluton Biella (Italy), Western Alps, (Masterarbeit)*. Switzerland: Institut für Geologie, Universität Bern. 73 p.

Compagnoni, R., Dal Piaz, G. V., Hunziker, G. C., Gosso, G., Lombardo, B., & Williams, P. F. (1977). The Sesia-Lanzo Zone, a slice of continental crust with Alpine high pressure–low temperature assemblages in the western Italian Alps. *Rendiconti Societa Italiana Mineralogia Petrologica, 33*, 281–334.

Condon, D., Schoene, B., Bowring, S., Parrish, R., McLean, N., Noble, S. & Crowley, Q. (2007). EARTHTIME: Isotopic tracers and optimized solutions for high-precision U–Pb ID-TIMS Geochronology. *American Geophysical Union, Fall Meeting, 2007*, #V41E–06.

Conticelli, S., Guarnieri, L., Farinelli, A., Mattei, M., Avanzinelli, R., Bianchini, G., et al. (2009). Trace elements and Sr–Nd–Pb isotopes of K-rich, shoshonitic, and calc-alkaline magmatism of the Western Mediterranean region: Genesis of ultrapotassic to calc-alkaline magmatic associations in a post-collisional geodynamic setting. *Lithos, 107*, 68–92.

Dal Piaz, G. V. (1999). The Austroalpine-Piemont nappe stack and the puzzle of western Alpine Thetys. *Memorie Scienca Geologica, 51*, 155–176.

Dal Piaz, G. V., Venturelli, G., & Scolari, A. (1979). Calc alkaline to ultrapotassic postcollisional volcanic activity in the internal Northwestern Alps. *Memorie Scienca Geologica, 32*, 1–16.

De Capitani, L., Fiorentini Potenza, M., Marchi, A., & Sella, M. (1979). Chemical and Tectonic contributions to the age and petrology of the Canavese and Sesia–Lanzo "porphyrites". *Atti Società Italiana di Scienze Naturali, 120*, 151–179.

Di Giulio, A., Carrapa, B., Fantoni, R., Gorla, L., & Valdisturlo, A. (2001). Middle Eocene to early Miocene sedimentary evolution of the western Lombardian segment of the South Alpine foredeep (Italy). *International Journal of Earth Science, 90*, 534–548.

Digel, S., & Ghent, E. D. (1994). Fluid mineral equilibrium in prehnite-pumpellyite to greenschist facies metabasites near Flin Flon, Manitoba, Canada: Implications for petrogenetic grids. *Journal of Metamorphic Geology, 12*, 467–477.

Dunkl, I. (2002). Trackkey: A windows program for calculation and graphical presentation of fission track data. *Computers and Geosciences, 28*, 3–12.

Fischer, H., & Villa, I. M. (1990). Erste K/Ar und 40Ar/39Ar-Hornblende-Mineralalter des Taveyannaz-Sandsteins. *Schweizerische Mineralogische Petrographische Mitteilungen, 70*, 73–75.

Frey, M. (1986). Very low-grade metamorphism of the Alps—an introduction. *Schweizerische Mineralogische Petrographische Mitteilungen, 66*, 13–27.

Frey, M., de Capitani, C., & Liou, J. G. (1991). A new petrogenetic grid for low-grade Metabasites. *Journal of Metamorphic Geology, 9*, 497–509.

Furrer, H., Schaltegger, U., Ovtcharova, M., & Meister, P. (2008). U-Pb zircon age of volcaniclastic layers in Middle Triassic platform carbonates of the Austroalpine Silvretta nappe (Switzerland). *Swiss Journal of Geoscience, 101*, 595–603.

Gerstenberger, H., & Haase, G. (1997). A highly effective emitter substance for mass spectrometric Pb isotope ratio determinations. *Chemical Geology, 136*, 309–312.

Giese, J., Seward, D., Stuart, F. M., Wüthrich, E., Gnos, E., Kurz, D., et al. (2010). Electrodynamic disaggregation: Does it affect apatite fission-track and (U–Th)/he analyses? *Geostandards and Geoanalytical Research, 34*, 39–48.

Gleadow, A. J. W. (1981). Fission-track dating methods: What are the real alternatives? *Nuclear Tracks, 5*, 3–14.

Handy, M.R., Babist, J., Rosenberg, C.L., Wagner, R., & Konrad, M. (2005). Decoupling and its relation to strain partitioning in continental lithosphere—insight from the periadriatic fault system (European Alps). In J.P. Brun, P. Cobbold & D. Gapais (Eds.), *Deformation mechanisms, Rheology and Tectonics* (Vol. 243, pp. 249–276). London: Geological Society of Special Publication.

Hrouda, F., & Lanza, R. (1989). Magnetic fabric in the Biella and Traversella stocks (Periadriatic line): Implications for the mode of emplacement. *Physics on the Earth and Planetary Interiors, 56*, 337–348.

Hurford, A. J., & Green, I. R. (1983). The zeta age calibration of fission track dating. *Isotope Geosciences, 1*, 285–317.

Hurford, A. J., & Hunziker, J. C. (1985). Alpine cooling history of the Monte Mucrone eclogites (Sesia-Lanzo Zone); fission-track evidence. *Schweizerische Mineralogische Petrographische Mitteilungen, 65*, 325–334.

Hurford, A. J., Hunziker, J. C., & Stockhert, B. (1991). Constraints on the late thermotectonic evolution of the Western Alps: Evidence for episodic rapid uplift. *Tectonics, 10*, 758–769.

Kapferer, N., Mercolli, I., & Berger, A. (2011). The composition and evolution of an Oligocene regolith on top of the Sesia-Lanzo Zone (Western Alps). *International Journal of Earth Science, 100*, 1115–1127.

Ketcham, R. A. (2005). Forward and inverse modeling of low-temperature thermochronometry data. *Reviews in Mineralogy and Geochemistry, 58*, 275–314.

Ketcham, R. A., Carter, A., Donelick, R. A., Barbarand, J., & Hurford, A. J. (2007). Improved modeling of fission-track annealing in apatite. *American Mineralogist, 92*, 799–810.

Krogh, T. E. (1973). A low contamination method for hydrothermal decomposition of zircon and extraction of U and Pb for isotopic age determination. *Geochimica et Cosmochimica Acta, 37*, 485–494.

Kübler, B. (1967). *La cristallinité de l'illite et les zones tout à fait supérieures du metamorphisme* (pp. 105–122). Colloque de Neuchâtel: Etages tectoniques.

Lanza, R. (1977). Palaeomagnetic data from the andesitic and lamprophyric dykes of the Sesia–Lanzo zone (Western Alps). *Schweizerische Mineralogische Petrographische Mitteilungen, 57*, 281–290.

Lanza, R. (1979). Paleomagnetic Data on the andesitic cover of the Sesia- Lanzo Zone (Western Alps). *Geologische Rundschau, 68*, 83–92.

Liou, J. C., Maruyama, S., & Cho, M. (1987). Very low-grade metamorphism of volcanic and volcaniclastic rocks: Mineral assemblages and mineral facies. In M. Frey (Ed.), *Low temperature metamorphism* (pp. 59–113). Glasgow: Blackie and Son.

Ludwig, K. R. (1980). Calculation of uncertainties of U–Pb isotope data. *Earth and Planetary Science Letters, 46*, 212–220.

Ludwig, K.R. (2005). Isoplot/Ex. V. 3. US geological survey open-file report.

Malaroda, R., Bertolami, G., Carraro, F., Friz, C., Govi, M., & Sacchi, R. (1966). *Carta Geologica d'Italia, Foglio 43, "Biella" 1:50,000* (2nd ed.). Roma: Service Geologica Italia.

Malusá, M. G., Philippot, P., Zattin, M., & Martin, S. (2006). Late stage of exhumation constrained by tructural, fluid inclusion and fission track analyses (Sesia–Lanzo unit, Western European Alps). *Earth and Planetary Science Letters, 243*, 565–580.

Malusá, M. G., Polino, R., Zattin, M., Bigazzi, G., Martin, S., & Piana, F. (2005). Miocene to Present differential exhumation in the Western Alps: Insights from fission track thermochronology. *Tectonics, 24*, 1–23.

Mattinson, J. M. (2005). Zircon U-Pb chemical abrasion ("CA-TIMS") method: Combined annealing and multi-step partial dissolution analysis for improved precision and accuracy of zircon ages. *Chemical Geology, 200*, 47–66.

McLean, N.M., Bowring J.F. & Bowring S.A. (2011). A algorithm for U–Pb isotope dilution data reduction and uncertainty propagation. *Geochemistry Geophysics Geosystems, 12*, Q0AA18.

Owen, J. P. (2008). Geochemistry of lamprophyres from the Western Alps, Italy: Implications for the origin of an enriched isotopic component in the Italian mantle. *Contribution to Mineralogy and Petrology, 155*, 341–362.

Pieri, M., & Groppi, G. (1981). Subsurface geological structure of the Po Plain. Progetto Finalizzato Geodinamica, Sottoprogetto "Modello Strutturale". *Publication Italian CNR, 144*, 1–13.

Puschnik, P. (2000). Hydrothermale Gangmineralisationen im Pluton Valle del Cervo (Region Piemont, Italien). *unpublished Diploma thesis,* Leoben, 109 p.

Reading, H.G. (1996). *Sedimentary environments: Processes, facies and stratigraphy*. (3rd edn.) Oxford: Blackwell Science, 688.

Robinson, D., & Bevins, R.E. (1999). Patterns of regional low-grade metamorphism in metabasites. In M. Frey & D. Robinson (Eds.), Low-Grade Metamorphism (pp. 143–168). Oxford: Blackwell Science.

Romer, R. L., Schärer, U., & Steck, A. (1996). Alpine and pre-Alpine magmatism in the root-zone of the Western Central Alps. *Contribution to Mineralogy and Petrology, 123*, 138–158.

Rossetti, P., Agangi, A., Castelli, D., Padoan, M., & Ruffini, R. (2007). The Oligocene Biella Pluton (Western Alps, Italy): New

insights on the magmatic versus hydrothermal activity in the Valsessera roof zone. *Periodico Mineralogia, 76*, 223–240.

Ruffini, R., (1995). Evidenze di attività vulcanica terziaria nelle Alpi Occidentali: Problemi ed ipotesi. *PhD thesis*, Università di Torino 160.

Ruffini, R., Polino, R., Callegari, E., Hunziker, J. C., & Pfeifer, H. R. (1997). Volcanic clasts rich turbidites of the Taveyanne sandstones from the Thônes syncline (Savoie France): Records for a tertiary postcollisonal volcanism. *Schweizerische Mineralogische Petrographische Mitteilungen, 77*, 161–174.

Schaltegger, U., Brack, P., Ovtcharova, M., Peytcheva, I., Schone, B., Stracke, A., et al. (2009). Zircon and titanite recording 1.5 million years of magma accretion, crystallization and initial cooling in a composite pluton (souther Adamello batholith, northern Italy). *Earth and Planetary Science Letters, 286*, 208–218.

Scheuring, B., Ahrendt, H., Hunziker, J. C., & Zingg, A. (1974). Paleobotanical and geochronological evidence for the Alpine age of the metamorphism in the Sesia-Zone. *Geologische Rundschau, 63*, 305–326.

Schlunegger, F., Melzer, J., & Tucker, G. E. (2001). Climate, exposed source-rock lithologies, crustal uplift and surface erosion: A theoretical analysis calibrated with data from the Alps/North Alpine Foreland Basin system. *International Journal of Earth Science, 90*, 484–499.

Schmid, S. M., Aebli, H. R., Heller, F., & Zingg, A. (1989). The role of the Periadriatic line in the tectonic evolution of the Alps. In D. Dietrich, M.P. Coward (Eds.), *Alpine tectonics* (Vol. 45, pp. 153–171). London: Geological Society of London Special Publication.

Schmid, S. M., Zingg, A., & Handy, M. (1987). The kinematics of movements along the Insubric Line and the emplacement of the Ivrea zone. *Tectonophysics, 135*, 47–66.

Schmitz, M. D., & Schoene, B. (2007). Derivation of isotope ratios, errors and error correlations for U–Pb geochronology using $^{205}Pb^{235}U(^{233}U)$-spike isotope dilution thermal ionization mass spectrometric data. *Geochemisty Geophysics Geosystems, 8*, Q08006.

Schoene, B., Crowley, J. L., Condon, D., Schmitz, M. D., & Bowring, S. A. (2006). Reassessing the uranium decay constants for geochronology using ID-TIMS U–Pb data. *Geochimica et Cosmochimica Acta, 70*, 426–445.

Siegesmund, S., Layer, P., Dunkl, I., Vollbrecht, A., Steenken, A., Wemmer, K. & Ahrendt, H. (2008). Exhumation and deformation history of the lower crustal section of the Val Strona di Omegna in the Ivrea zone, Southern Alps. In S. Siegesmund, B. Fügenschuh, & N. Froitzheim (Eds.), *Tectonic aspects of the Alpine–Dinaride–Carpathians system* (Vol. 298, pp. 45–68). London: Geological Society of London Special Publication.

Simon, J. I., Renne, P. R., & Mundil, R. (2008). Implications of pre-eruptive magmatic histories of zircons for U–Pb geochronology of silicic extrusions. *Earth and Planetary Science Letters, 266*, 182–194.

Sinclair, H. D. (1992). Turbidite sedimentation during alpine thrusting: The Taveyannaz sandstones of eastern Switzerland. *Sedimentology, 39*, 837–856.

Spiegel, C., Kuhlemann, J., Dunkl, I., & Frisch, W. (2001). Paleogeography and catchment evolution in a mobile orogenic belt: The Central Alps in Oligo–Miocene times. *Tectonophysics, 341*, 33–47.

Stacey, J. S., & Kramers, J. D. (1975). Approximation of terrestrial lead isotope evolution by a two-stage model. *Earth and Planetary Science Letters, 26*, 207–221.

Tommasini, S., Avanzinelli, R., & Conticelli, S. (2011). The Th/La and Sm/La conundrum of the Tethyan realm lamproites. *Earth and Planetary Science Letters, 301*, 469–478.

Van Marcke de Lumen, G., & Vander Auwera, J. (1990). Petrogenesis of Traversella diorite (Piemonte Italy): A major trace element and isotopic (O, Sr) model. *Lithos, 24*, 121–136.

Venturelli, G., Thorpe, R. S., Dal Piaz, G. V., Del Moro, A., & Potts, P. J. (1984). Petrogenesis of calc-alkaline, shoshonitic and associated ultrapotassic Oligence volcanic rocks from the Northwestern Alps, Italy. *Contribution to Mineralogy and Petrology, 86*, 209–220.

Vessel, R. K., & Davies, D. K. (1981). Non-marine sedimentation in an active fore-arc basin. In: Recent and ancient non-marine depositional environments. *SEPM Special Publication, 31*, 31–45.

Vuagnat, M. (1983). Les grès de Taveyanne et roches similaires: Vestiges d'une activité magmatique tardi-alpine. *Memorie della Società Geologica Italiana, 26*, 39–53.

Wagner, G. A., & Reimer, G. M. (1972). Fission track tectonics: The tectonic interpretation of fission track apatite ages. *Earth and Planetary Science Letters, 14*, 263–268.

Wissmann, K., (1985). Die Insubrische Linie den tertiären Magmatiten NW'Biella, Provinz Vercelli, italienische Westalpen. *Diploma Thesis*, University of Göttingen, Germany, 133.

Zanoni, D., Bado, L., Spalla, M. I., Zucali, M., & Gosso, G. (2008). Structural analysis of the Northeastern margin of the tertiary intrusive stock of Biella (Western Alps, Italy). *Bolletino della Societa Geologica Italiania, 127*, 125–140.

Zanoni, D., Spalla, M. I., & Gosso, G. (2010). Structure and PT estimates across late-collisional plutons: Constraints on the exhumation of Western Alpine continental HP units. *International Geological Reviews, 52*, 1244–1267.

Zingg, A., & Hunziker, J. C. (1990). The age of movements along the Insubric line west of Locarno (N Italy and S Switzerland). *Eclogae Geologicae Helvetica, 83*, 629–644.

Zingg, A., Hunziker, J. C., Frey, M., & Ahrendt, H. (1976). Age and degree of metamorphism of the Canavese zone of the sedimentary cover of the Sesia zone. *Schweizerische Mineralogische Petrographische Mitteilungen, 56*, 361–375.